



Dielectric properties of electrolyte solutions in polymeric nanofiltration membranes

Miguel Montalvillo^{a,b}, Verónica Silva^{a,b}, Laura Palacio^{a,b}, Antonio Hernández^{a,b,*}, Pedro Prádanos^{a,b}

^aDepartamento de Física Aplicada, Facultad de Ciencias, Universidad de Valladolid, Real de Burgos s/n, 47071 Valladolid, Spain

^bSurface and Porous Materials (SMAP), UA CSIC-UVA, R&D Building, 47071 Valladolid, Spain
Tel. +34 983423134; email: tonhg@termo.uva.es

Received 28 May 2010; Accepted 14 August 2010

ABSTRACT

In this work a nanofiltration membrane immersed in an electrolyte solution has been studied using impedance spectroscopy. In this technique the membrane is in contact with the same concentration at both sides, therefore there is not any ion transport through the membrane and, thus, it is possible to obtain electric and dielectric properties that would help to model the nanofiltration process. Results allow obtaining the electrical properties of the whole system assumed as consisting in an equivalent electric circuit. Three relaxation times can be identified and modeled with the aim of understanding the behavior of the solution inside the pores as a function of concentration. The pore permittivity decreases with increasing concentration due to confinement effects, while the conductivity inside the pores increases rapidly for high concentrations due to the easy penetration of the ions into the pores.

Keywords: Impedance spectroscopy; Nanofiltration; Conductivity; Permittivity; Dielectric properties

1. Introduction

Nanofiltration membranes have extraordinary characteristics that make them able to reject multivalent ions and transmit small uncharged solutes and low charged ions. Therefore, the characterization of the electric and dielectric behavior of the membrane is one of the most important aspects to study. Some experimental techniques have been applied with this aim like streaming potential [1,2], membrane potential (MP) [3,4] and impedance spectroscopy (IS) [5,6]. With these methods it is basically possible to obtain the charge developed in the membrane by the ions, the mobility of the ions and the permittivity inside the pores. Moreover, some models have been developed to explain the extra rejection produced in nanofiltration due

to dielectric effects inside the pores of the membrane [7,8]. This theoretical description usually keeps the permittivity inside the pore as a fitting parameter. This procedure gives, in most cases, reasonable values (permittivities below the free solution one) [9,10]. However, in certain conditions the fitted permittivity reaches values that are difficult to understand (higher than the solution outside the pores) [11,12]. This makes very interesting an independent measurement of pore permittivity of nanofiltration membranes.

The impedance spectroscopy (IS) technique is typically used to study the electrical properties of complex materials [5,6]. The operation mode consists in introducing an electrical signal and performing a frequency scanning, and measuring the impedance of the system at such different signal frequencies. With IS, it is possible to obtain the different contributions of each layer of the membrane and also to characterize the electrical double layer. In this technique the system is modeled by an

*Corresponding author.

equivalent electrical circuit from which it is possible to obtain the resistance and capacitance of each layer [13].

In this work, IS has been applied to a commercial NF membrane in a wide range of KCl concentrations. The permittivity (ϵ_p) and conductivity (κ_p) inside the pores of this membrane are the target magnitudes to be obtained.

2. Theory and methods

In our case the membrane system is composed by:

ELECTRODE | electrolyte | MEMBRANE | electrolyte | ELECTRODE

Then, experimental IS measurements give us information on the conductance (G) and capacitance (C) of the complete system. In this configuration, several layers and polarization interfaces can be identified. All these layers have different electrical properties and consequently different relaxation times. In a general way, the system can be modeled using an extension of the Maxwell–Wagner theory where the whole complex capacitance for an N -layers system is obtained [14] by

$$C^*(\omega) = C_{N,h} + \sum_{i=1}^{N-1} \frac{C_{i,l} - C_{i,h}}{1 + (j\omega\tau_i)^{1-\alpha_i}} - j \frac{G_{11}}{\omega} \quad (1)$$

where $\tau_i = 1/2\pi f_i$ and f_i is the frequency at the maximum value in the corresponding semicircle in the Nyquist plot (or the inflection point in the C or G versus frequency plots), ω is the angular frequency, $C_{N,h}$ is the conductance at infinite frequency, $C_{i,l}$ and $C_{i,h}$ are the conductances for each relaxation time at low and high frequency respectively. The α_i constant is a distribution factor characterizing the spread of relaxation time [15].

In the case of multilayer systems there are some links in Eq. (1):

$$C_{i,h} + C_{(i+1),l} \quad \text{for } i = 1, \dots, N-1 \quad (2)$$

$$G_{i,h} + G_{(i+1),l} \quad \text{for } i = 1, \dots, N-1 \quad (3)$$

Using experimental results (left side in Eq. (1)) it is possible to identify the dielectric parameter $C_{N,h}$, $G_{1,l}$, $C_{i,h}$, $G_{i,h}$ and α_i .

In order to quantify the dielectric properties in the membrane system, the parameters of membrane-electrolyte interface can be estimated from the dielectric parameters presented above and the procedure presented by Li and Zhao [16]. They characterize an equivalent circuit for the whole range of frequencies, representing a series combination of capacitance and resistance

Table 1

Relation between phase and dielectric parameters [16] (in order to get the permittivity and conductivity in the membrane pores, Eq. (1.5)–(1.8) must be used)

$$\omega_i = \frac{G_h - G_l}{C_l - C_h} = 2\pi f_i \quad (1.1)$$

$$B = \omega_i + \frac{G_h}{C_h} \quad (1.2)$$

$$D = \sqrt{B^2 - 4 \frac{G_l \omega_i}{C_h}} \quad (1.3)$$

$$a = \frac{B - D}{2} \quad b = B - a \quad (1.4)$$

$$C_m = C_h \frac{D}{\omega_i - a} \quad \epsilon_m = C_m \frac{\Delta x}{S \epsilon_0} \quad (1.5)$$

$$C_b = C_h \frac{D}{b - \omega_i} \quad \epsilon_b = C_b \frac{L}{S \epsilon_0} \quad (1.6)$$

$$G_m - a C_m \quad \kappa_m = G_m \frac{\Delta x}{S} \quad (1.7)$$

$$G_b = b C_b \quad \kappa_b = G_b \frac{L}{S} \quad (1.8)$$

The sub-indexes h and l in the table refer to the high and low frequencies in the same relaxation time, i refers to the i th relaxation and m and b refer to the property inside and outside of the membrane. L is the distance from electrode to electrode minus the membrane thickness, Δx , and S is the area of the sample.

in parallel. When this procedure is applied only in the frequency range corresponding to the relaxation time of the solution inside the membrane, the phase parameters can be obtained according to the equations presented in Table 1.

3. Experimental

3.1. Membrane and electrolytes

In this study a flat sheet commercial polyamide nanofiltration membrane, Desal HL manufactured by Osmonics SA (Vista, CA, USA) was used. According to the manufacturers, it has a MWCO between 150 and 300 g/mol, a range of pH of 3–9 and a maximum operation temperature of 50°C. We will assume a mean pore radius of 0.48 nm as obtained by Hussain et al. [17] from retention experiments of uncharged solutes.

The non-woven support of the membrane was mechanically peeled off the membrane. Before starting the experiments, the membrane was left during 24 h in the cell with milli-Q deionized water to remove air and impurities from the membrane.

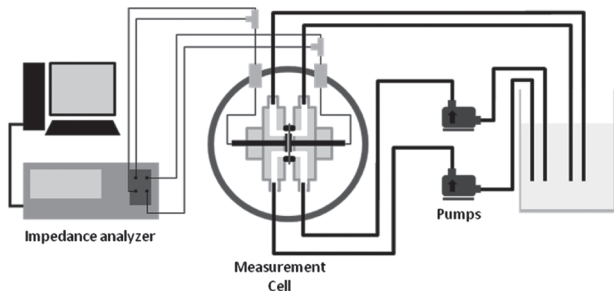


Fig. 1. Schematic representation of the impedance measurement system.

KCl was used to prepare seven concentrations with milli-Q deionized water in a range from 10^{-2} to 10 mol/m^3 . Once the membrane was placed in the system, the solution was kept flowing on both sides of the membrane at the same tangential speed during a few minutes needed to equilibrate the membrane with the solution and to stabilize the measurements.

3.2. Impedance spectroscopy

Here a Solartron 1260 was used for the impedance measurements for frequencies ranging from 10 MHz to 10 mHz and under 10–50 mV applied AC voltage. In these experiments seven points per decade were used obtaining a total of 64 points, this number of points is enough to appreciate all relaxation times in a reasonable operation time of about 1 h. The equipment is controlled by the acquisition and control software provided also by Solartron Analytical.

The measurement cell and the whole arrangements were designed by us. The cell has two identical hemi-cell of methacrylate of $10 \times 18 \text{ cm}^2$ active area, with two flat and circular Ag/AgCl electrodes of 38 mm of diameter. The distance from electrode to electrode is approximately 2 mm. Both semi-cells were placed inside a stainless steel vessel that acts as a Faraday shield and isolates the system from any external electromagnetic field that could interfere with the measurement. The system and connections with the impedance analyzer are shown in Fig. 1. During measurements, the solution was continuously flowing tangentially on both sides of the cell at a flux of 0.6 L/min at $25 \pm 1^\circ\text{C}$ of temperature.

4. Results and discussion

4.1. Dielectric behavior of KCl in the membrane system

For the analysis of the experimental results, the equivalent circuit presented in Fig. 2 was used to obtain

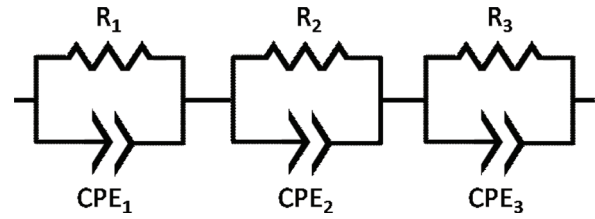


Fig. 2. Equivalent circuit used in the modeling of Impedance results. CPE stands for a constant phase element (a capacitance where there are non-uniformities due to fluctuations in thickness, surface roughness, etc).

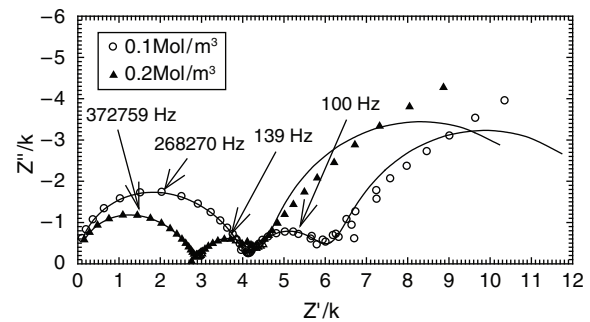


Fig. 3. Nyquist diagram for 1 and 0.1 mol/m^3 of KCl. Symbols are experimental results and continuous lines are the modeling results. Some frequencies are superimposed.

the dielectric parameters of Eq. (1). In the studied system, three relaxation times can be recognized and observed in the Nyquist plot shown in Fig. 3 as an example.

The following correspondences were determined by comparison between the results at the different studied concentrations and also comparing with the system response without membrane:

- (1) The first semicircle represents the solution outside the membrane flowing through the cell; it appears also in the measurements for the same concentrations without membrane and in the same range of frequencies.
- (2) The second semicircle only appears in the measurements with membrane in the system, so it is attributable to the solution inside the pores. These properties are different from those outside them.
- (3) The last semicircle, which is less defined, appears in all kinds of measurements and changes with the intensity of the applied electric field. This relaxation should be caused by the resistance to transport due to the accumulation of the transported ions on the electrode surface (electrode polarization).

The model was solved for $C_{N,h}$, $G_{1,l}$, $C_{i,h}$, $G_{i,h}$ and α_i for each relaxation presented in Section 2.1. $C_{N,h}$ was set

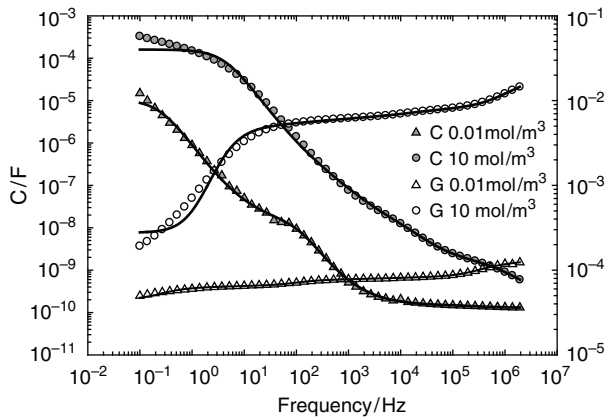


Fig. 4. Frequency dependence of the capacitance and conductance for 10^{-2} and 10 mol/m³ of KCl concentrations. Symbols are experimental results and continuous lines are the modeling results.

equal to 130 pF for all concentrations since this is the value that all concentrations reach after extrapolation at infinite frequency. The parameters were easily fitted by testing a large number of initial guesses which led to the same fitted values. In all cases (β was very close to 1, especially for the central semicircle the worst circumstances gave a deviation from 1 lower than a 2%). The resulting dependences of capacitance and conductance on frequency are shown as solid lines in Fig. 4 for the higher and lower concentrations studied.

The permittivity and conductivity obtained from the first semicircle are, within the error range, equal to those of free bulk solution without any clear tendency with concentrations for permittivity.

4.2. Permittivity inside NF pores

The resulting membrane capacitance (C_m) obtained using Eq. (1.5) is an overall value. Thus the corresponding relative permittivity, ϵ_m , includes the membrane material, ϵ_d , and the solution inside the pores, ϵ_p , so it could be called wet membrane permittivity. The relation between these three permittivities is given by means of the membrane porosity, A_k

$$\epsilon_m = \epsilon_p A_k + (1 - A_k) \epsilon_d \quad (4a)$$

The same situation occurs for the conductivity

$$k_m = k_p A_k + (1 - A_k) k_d \quad (4b)$$

The permittivity and conductivity of the filled pores (ϵ_p and κ_p) can be obtained, assuming that both

magnitudes for the dry polymer (ϵ_d and κ_d) are negligible compared to the solution ones. Then, Eqs. (4) become

$$\epsilon_m = C_m \frac{\Delta x}{S \epsilon_0} = \epsilon_p A_k \quad (5a)$$

$$\kappa_m = C_m \frac{\Delta x}{S} = \kappa_p A_k \quad (5b)$$

The ratio $\Delta x/A_k$ can be determined by using the Hagen–Poiseuille equation

$$\frac{\Delta x}{A_k} = \frac{r_p^2}{\beta \eta_p L_w} \quad (6)$$

where the water permeability was experimentally measured being $2.78 \cdot 10^{-11}$ m/sPa. The constant β should be 8 for cylindrical geometries or 3 for slit-shaped pores. It has been proved that the solution viscosity is enhanced inside nanometric pores due to the confinement effect. Wesolowska et al. [18], give a method to quantify this increase in viscosity, that applied to this membrane gives η_p is $7 \cdot 10^{-3}$ Pa s. Finally, the permittivity and conductivity inside the membrane pores were calculated as

$$\epsilon_p = \frac{C_m r_p^2}{S \epsilon_0 \beta \eta_p L_w} \quad (7a)$$

$$\kappa_p = \frac{G_m r_p^2}{S \beta \eta_p L_w} \quad (7b)$$

It is worth noting that in Eqs. (7), L_w is the overall water permeability (for the membrane without the non-woven support that was peeled off) while the value taken for r_p was obtained from retention experiments. Thus this pore radius corresponds to the active layer of the membrane. Due to these assumptions it is clear that the so obtained ϵ_p and κ_p should correspond to the active layer provided that the contribution to permeability and to the dielectric response of the porous layers retained with the membrane were negligible. Actually these assumptions seem reasonable mainly if we look to the almost perfectly semicircular shape corresponding to the second relaxation in the Nyquist plot.

In Fig. 5 both parameters were represented against the concentration for both geometries. These so obtained dielectric constants inside the pores are lower than those outside the pores, in agreement with the dielectric theory [19].

The pore conductivity increases with concentration while the pore permittivity decreases with concentration as could be expected. The conductivity inside and outside the pores are compared in Fig. 6.

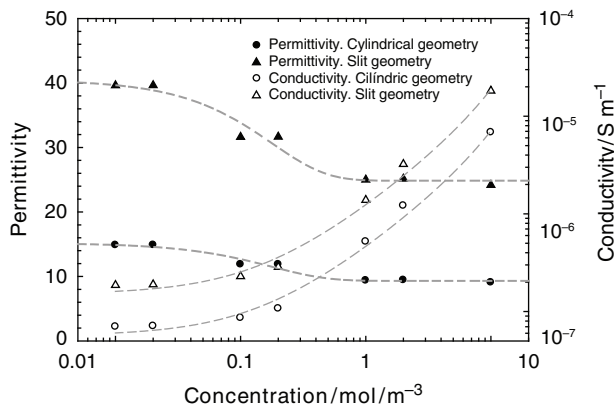


Fig. 5. Permittivity and conductivity inside the membrane pores as function of concentration.

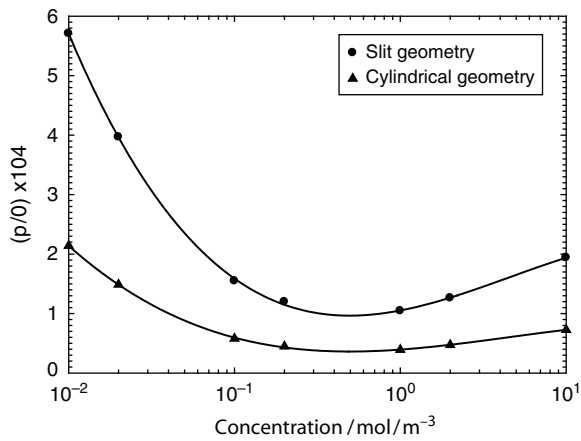


Fig. 6. Conductivity inside the membrane pores compared with the conductivity outside them.

Note that pore conductivity is always lower than outside the membrane and this reduction increases with concentration up to a plateau at high concentrations. A similar plot for the pore permittivity is not pertinent as far as the permittivity outside the membrane is substantially independent of concentration. In any case the pore permittivity is smaller than outside the membrane and decreases even more with concentration until a plateau is reached at high concentrations.

5. Conclusions

The IS method allows a separation of the different relaxation processes appearing in a complex membrane system.

A comparison of the measurements with and without the membrane, under different applied voltages and

with differently concentrated electrolytical solutions allows identifying the relaxation processes with the different contributions of the phases and interfaces in the membrane system.

Experimental results can be fitted to obtain the conductivity and permittivity of the membrane as functions of concentration. These data should improve the modelization of nanofiltration processes.

Acknowledgements

Authors thank the Junta de Castilla y León for financing of this research through the projects BU-03-C3 (INNOVIN-ALCOHOLGRADE) and Grupos de Excelencia-GR18, along with the Ministerio de Educación y Ciencia (Plan Nacional de I+D+i) through CTQ2009-07666 and MAT2008-00619.

Symbols

A_k	—	Porosity of the active layer
a, b, B, D	—	Parameters defined in Table 1
C	—	Capacitance
f	—	Frequency
G	—	Conductance
j	—	Imaginary number
L	—	Distance from electrode to electrode minus the membrane thickness
L_w	—	Water permeability
S	—	Membrane area
r_p	—	Pore radius

Greeks

α	—	Distribution factor of relaxation times
β	—	Factor defining pore geometry
ϵ	—	Permittivity
ϵ_0	—	Vaccum permittivity
η	—	Viscosity
κ	—	Conductivity
τ	—	Relaxation time
ω	—	Angular frequency
Δx	—	Active layer thickness

Subscripts

d	—	Dry membrane
h	—	High frequency
l	—	Low frequency
m	—	Membrane
p	—	Pores

References

- [1] P. Fievet, M. Sbai, A. Szymczyk, C. Magnenet, C. Labbez and A. Vidonne, A new tangential streaming potential setup for the electrokinetic characterization of tubular membranes, *Sep. Sci. Technol.*, 39 (13) (2004) 2931.
- [2] F. Martínez, A. Martín, J. Malfeito, L. Palacio, P. Prádanos, F. Tejerina and A. Hernández, Streaming potential through and on ultrafiltration membranes: Influence of salt retention, *J. Membr. Sci.*, 206 (1–2) (2002) 431.
- [3] P. Fievet, B. Aoubiza, A. Szymczyk and J. Pagetti, Membrane potential in charged porous membranes, *J. Membr. Sci.*, 160 (2) (1999) 267.
- [4] W.J. Shang, X.L. Wang and Y.X. Yu, Theoretical calculation on the membrane potential of charged porous membranes in 1-1, 1-2, 2-1 and 2-2 electrolyte solutions, *J. Membr. Sci.*, 285 (1–2) (2006) 362.
- [5] V. Freger and S. Bason, Characterization of ion transport in thin films using electrochemical impedance spectroscopy: I. Principles and theory, *J. Membr. Sci.*, 302 (1–2) (2007) 1.
- [6] S. Bason, Y. Oren and V. Freger, Characterization of ion transport in thin films using electrochemical impedance spectroscopy: II: examination of the polyamide layer of RO membranes, *J. Membr. Sci.*, 302 (1–2) (2007) 10.
- [7] A.E. Yaroshchuk, Dielectric exclusion of ions from membranes, *Adv. Colloid Interface Sci.*, 85 (2–3) (2000) 193.
- [8] A.E. Yaroshchuk, Non-steric mechanisms of nanofiltration: superposition of Donnan and dielectric exclusion, *Sep. Purif. Technol.*, 22–23 (1–3) (2001) 143.
- [9] A. Szymczyk, M. Sbai, P. Fievet and A. Vidonne, Transport properties and electrokinetic characterization of an amphoteric nanofilter, *Langmuir*, 22 (8) (2006) 3910.
- [10] A. Szymczyk and P. Fievet, Investigating transport properties of nanofiltration membranes by means of a steric, electric and dielectric exclusion model, *J. Membr. Sci.*, 252 (1–2) (2005) 77.
- [11] S. Bouranene, P. Fievet and A. Szymczyk, Investigating nanofiltration of multi-ionic solutions using the steric, electric and dielectric exclusion model, *Chem. Eng. Sci.*, 64 (2009) 3789.
- [12] S. Déon, P. Dutournié, L. Limousy and P. Bourseau, Transport of salt mixtures through nanofiltration membranes: numerical identification of electric and dielectric contributions, *Sep. Purif. Technol.*, 69 (2009) 225.
- [13] J. Benavente, J.M. García, R. Riley, A.E. Lozano and J. de Abajo, Sulfonated poly(ether ether sulfones): characterization and study of dielectrical properties by impedance spectroscopy, *J. Membr. Sci.*, 175 (1) (2000) 43.
- [14] Y. Kita, Dielectric-relaxation in distributed dielectric layers, *J. Appl. Phys.*, 55 (10) (1984) 3747.
- [15] K. Asami, Characterization of heterogeneous systems by dielectric spectroscopy, *Prog. Polym. Sci.*, 27 (8) (2002) 1617.
- [16] Y.H. Li and K.S. Zhao, Dielectric analysis of nanofiltration membrane in electrolyte solutions: influences of electrolyte concentration and species on membrane permeation, *J. Colloid Interface Sci.*, 276 (1) (2004) 68.
- [17] A.A. Hussain, S.K. Nataraj, M.E.E. Abashar, I.S. Al-Mutaz and T.M. Aminabhavi, Prediction of physical properties of nanofiltration membranes using experiment and theoretical models, *J. Membr. Sci.*, 310 (1–2) (2008) 321.
- [18] K. Wesolowska, S. Koter and M. Bodzek, Modelling of nanofiltration in softening water, *Desalination*, 162 (2004) 137.
- [19] S. Senapati and A. Chandra, Dielectric constant of water confined in a nanocavity, *J. Phys. Chem. B*, 105 (22) (2001) 5106.